Science Press

Online system, http://www.scar.ac.cn
Sciences in Cold and Arid Regions
2011, 3(1): 0041–0050
DOI: 10.3724/SP.J.1226.2011.00041

Estimation of ground heat flux and its impact on the surface energy budget for a semi-arid grassland

JinQing Zuo [1,2], JieMin Wang [3], JianPing Huang [1*], WeiJing Li [2], GuoYin Wang [1], HongLi Ren [2]

1. Key Laboratory for Semi-Arid Climate Change of the Ministry of Education, College of Atmospheric Sciences, Lanzhou University, Lanzhou, Gansu 730000, China
2. Laboratory for Climate Studies, China Meteorological Administration, Beijing 100081, China
3. Cold and Arid Regions Environmental and Engineering Research Institute, Chinese Academy of Sciences, Lanzhou, Gansu 730000, China

*Correspondence to: Dr. JianPing Huang, Professor of Key Laboratory for Semi-Arid Climate Change of the Ministry of Education, College of Atmospheric Sciences, Lanzhou University, No. 222, South Tianshui Road, Lanzhou, Gansu 730000, China. Email: hjp@lzu.edu.cn

Received: 18 August 2010   Accepted: 14 November 2010

ABSTRACT

Three approaches, *i.e.*, the harmonic analysis (HA) technique, the thermal diffusion equation and correction (TDEC) method, and the calorimetric method used to estimate ground heat flux, are evaluated by using observations from the Semi-Arid Climate and Environment Observatory of Lanzhou University (SACOL) in July, 2008. The calorimetric method, which involves soil heat flux measurement with an HFP01SC self-calibrating heat flux plate buried at a depth of 5 cm and heat storage in the soil between the plate and the surface, is here called the ITHP approach. The results show good linear relationships between the soil heat fluxes measured with the HFP01SC heat flux plate and those calculated with the HA technique and the TDEC method, respectively, at a depth of 5 cm. The soil heat fluxes calculated with the latter two methods well follow the phase measured with the HFP01SC heat flux plate. The magnitudes of the soil heat flux calculated with the HA technique and the TDEC method are close to each other, and they are about 2 percent and 6 percent larger than the measured soil heat flux, respectively, which mainly occur during the nighttime. Moreover, the ground heat fluxes calculated with the TDEC method and the HA technique are highly correlated with each other (R^2 = 0.97), and their difference is only about 1 percent. The TDEC-calculated ground heat flux also has a good linear relationship with the ITHP-calculated ground heat flux (R^2 = 0.99), but their difference is larger (about 9 percent). Furthermore, compared to the HFP01SC direct measurements at a depth of 5 cm, the ground heat flux calculated with the HA technique, the TDEC method, and the ITHP approach can improve the surface energy budget closure by about 6 percent, 7 percent, and 6 percent at SACOL site, respectively. Therefore, the contribution of ground heat flux to the surface energy budget is very important for the semi-arid grassland over the Loess Plateau in China. Using turbulent heat fluxes with common corrections, soil heat storage between the surface and the heat flux plate can improve the surface energy budget closure by about 6 to 7 percent, resulting in a closure of 82 to 83 percent at the SACOL site.

Keywords: soil heat flux; harmonic analysis; TDEC method; self-calculating heat flux plate; surface energy budget

1. Introduction

The impacts of human activities and land cover changes on the climate, and the regional climate responses to global environment change, are both results of the energy and mass exchanges between the surface and the atmosphere. Studies of these exchanges will help to further elucidate the energy and mass circulations of regional climate systems and regional climate changes. Total energy conservation is a major constraint in the land-atmosphere energy exchange process. However, observations in recent decades have shown that turbulent heat fluxes (the sum of sensible heat flux and latent heat flux) calculated with the most advanced eddy covariance technique are typically only about 70 to 90 percent of the surface available energy (the difference between net radiation and ground heat flux). In addition, lack of surface energy budget closure has been found in almost all of the studied flux sites (*e.g*., Wilson *et al*., 2002; Tanaka *et al.*, 2003; Culf *et al*., 2004; Yang *et al.*, 2004a; Li *et al*., 2005; Oncley *et al*., 2007). This imbalance problem must be solved over time because surface energy conservation is the basic principle for the land module in all of the atmospheric circulation models. An imbalance of greater than 10 percent is not acceptable for model testing and further development, especially for the land model. Moreover, the main technique for many applications,—the satellite retrieval of surface evapotranspiration that is used in water resource management—is also based on the surface energy conservation principle. In addition, the retrieval results must be tested with in-situ measurements. Therefore, surface energy budget closure has been used to characterize the quality of turbulent fluxes measured with the eddy covariance technique.

Recent studies have found that the correct determination of heat storage within the soil-vegetation-atmosphere system is a key factor in the solution of the surface energy imbalance (Ochsner *et al*., 2007; Foken, 2008). As a component of the surface energy balance, the ground heat flux (soil heat flux at the surface) plays an important role in the surface energy budget; its accurate estimation can improve the surface energy budget closure significantly, especially over surfaces with bare soil or sparse vegetation (Heusinkveld *et al*., 2004). This component is usually measured directly with a soil heat flux plate buried at a certain depth below the ground surface (such as depths of 5–10 cm), or derived from multi-level measurements of soil temperature and soil moisture. Because of the large gradient and significant phase difference (in vertical) of the soil temperature and soil heat flux, the accurate estimation of ground heat flux from measurements of soil temperature and soil moisture has been of wide concern in recent years (for review, refer to Zhang *et al*., 2004).

At present, there are several approaches to estimate the ground heat flux from observations, such as the common integral method which involves soil temperature measurements, and the calorimetric method which involves heat flux plate measurement (Liebethal *et al.*, 2005); the harmonic analysis (HA) technique (Horton *et al*., 1983); the empirical method (Zhang *et al*., 2006); and the method considering soil thermal conduction and convection (Fan and Tang, 1994; Gao *et al.*, 2003). Measurements with heat flux plates could be quite erroneous in magnitude because it is usually difficult to calibrate them accurately (van Loon *et al*., 1998). This would result in significant uncertainty in estimating ground heat flux with the calorimetric method involving heat flux plate measurement (hereinafter referred to as the ITHP approach). Jacobs *et al*. (2007) found that the HA technique has better accuracy than the ITHP approach in the estimation of ground heat flux. However, the HA technique assumes a vertical homogeneous soil, which may be far from the reality. In order to deal with these problems, Yang and Wang (2008) recently developed an integral method that is not sensitive to the soil thermal conductivity, which was named thermal diffusion equation and correction (TDEC). Moreover, in order to eliminate errors due to the changing thermal conductivity of the environment, a new type of heat flux plate with an in-situ self-calibrating function (model HFP01SC) has been recently developed by Hukseflux Thermal Sensors, Delft, The Netherlands. Van Loon *et al*. (1998) showed through laboratory testing that this type of heat flux plate has an accuracy within 5 percent, and field comparisons also demonstrated that its accuracy had been improved significantly (Cobos and Baker, 2003; Ochsner *et al*., 2006). This indicates that the ITHP approach involving an HFP01SC self-calibrating heat flux plate may be one of the most reliable and effective methods of estimating ground heat flux.

Since the TDEC method is a relatively new approach to estimate ground heat flux, to date there is no report about its application to surface energy budget study. Moreover, the effectiveness of the HFP01SC self-calibrating procedure needs more field tests over different types of surfaces. Therefore, in this study three approaches—the HA technique, the TDEC method, and the ITHP approach involving an HFP01SC self-calibrating heat flux plate—are evaluated to estimate ground heat flux by using observations from the Semi-Arid Climate and Environment Observatory of Lanzhou University (SACOL). Furthermore, the impacts of ground heat flux estimated with the above approaches on the surface energy budget closure will be assessed for a semi-arid grassland over the Loess Plateau of China.

2. Materials and methods

2.1. Experimental set-up

SACOL is located in the Loess Plateau mesa region in central Gansu (35°57′N, 104°08′E, elevation 1,966 m), which has a semi-arid climate. According to the Chinese Soil Classification System (1995), the soil type of this region is Sierozem. This region is a natural desert grassland with species of *Stipa bungeana*, *Artemisia frigida*, and *Leymus secalinu*. More details about SACOL can be found in a report by Huang *et al*. (2008).

The in-situ measurements used in this study mainly include soil temperature, soil moisture (soil water content), soil heat flux, and radiation fluxes with a sampling interval of 10 minutes. The soil temperature measurements were performed at depths of 2, 5, 10, 20, 50, and 80 cm (STP01-L, Hukseflux) and soil water content at depths of 5, 10, 20, 40, and 80 cm (CS616-L, Campbell). The soil heat flux was measured with a self-calibrating soil heat flux plate (HFP01SC-L, Hukseflux) at a depth of 5 cm. In addition, the upward and downward shortwave radiation fluxes were measured with a pyranometer (CM21, Kipp & Zonen), and the upward and downward longwave radiation fluxes with a pyrgeometer (CG4, Kipp & Zonen) at a height of 1.5 m above the ground surface. The surface temperature (T_{sfc}) was derived from the longwave radiation components as follows:

$$T_{sfc} = \left(\frac{R_{LW}^{\uparrow} - \left(1-\varepsilon_g\right) R_{LW}^{\downarrow}}{\varepsilon_g \sigma} \right)^{1/4} \quad (1)$$

where $R_{LW}^{\uparrow}$ and $R_{LW}^{\downarrow}$ are the upward and downward longwave radiation fluxes (W/m^2); the surface emissivity ε_g is set to be 0.98 empirically; and the Stefan-Boltzmann constant $\sigma = 5.67\times10^{-8}$ W/(m^2·K^4).

The turbulent heat fluxes (including sensible and latent heat fluxes) used to assess the surface energy budget closure were calculated from the measurements from the eddy covariance system. This system mainly consists of a three-axis sonic anemometer (CSAT3, Campbell) and an open-path infrared CO_2/H_2O analyzer (LI7500, LI-COR) at a height of 3.0 m above the ground surface. The sampling interval of raw data was 10 Hz and the averaging interval was 30 minutes for the calculation of turbulent fluxes. Before acquiring the turbulent fluxes, the data were processed with an automated quality assurance and quality control (QA/QC) procedure of eddy covariance measurements. For more information about the QA/QC procedure of turbulent fluxes, please refer to the work given by Zuo *et al.* (2009).

2.2. Principle of the self-calibrating heat flux plate

The HFP01SC self-calibrating heat flux plate is a new type of plate developed by Hukseflux Thermal Sensors, Delft, The Netherlands. This type of plate is 5 mm in thickness and 80 mm in diameter, and has a thermal conductivity (λ_m) of 0.8 W/(m·K). Unlike other types of heat flux plates, the HFP01SC has a film resistor covering its upper face. This resistor is used to generate a well known heat flux, ϕ, through the plate; then the self-calibrating procedure can be achieved by quantifying the response of the heat flux plate to the heating (Hukseflux Thermal Sensors, 1999). In an idealized scenario (*i.e.*, no gap and no difference of thermal conductivity between the soil and the plate), half of the heat flux, $\phi/2$, would pass upward into the surrounding medium and the other $\phi/2$ would pass downward through the plate. In reality, for a self-calibrating heat flux plate installed in soil, the actual flux through the plate caused by the heating, ϕ_h, will generally not be equal to $\phi/2$ due to the inconsistency of the thermal conductivity between the soil and the plate. The ratio of the actual flux to the ideal flux, $\phi_h/(\phi/2)$, is a measure of the heat flow distortion during heating and is defined as the calibration constant. Then the heat flux measured with the plate with the heater turned off can be calibrated in-situ as follows:

$$\frac{G_r}{G_m} = \frac{\phi_h}{\phi/2} \quad (2)$$

where G_r is the actual soil heat flux through the soil, which is the final output of the self-calibrating heat flux plate (W/m^2), and G_m the soil heat flux measured with the plate (W/m^2).

The HFP01SC heat flux plate was buried at a depth of 5 cm at the SACOL site. The ground heat flux in this site can be estimated by summing of the HFP01SC measurements ($G_{Obs,5}$) and the soil heat storage between the ground surface and the heat flux plate as follows:

$$G_{ITHP,0} = G_{Obs,5} + \frac{\rho_s c_s}{\Delta t} \sum_{z=5cm}^{z=0} \left[T\left(z_i, t+\Delta t\right) - T\left(z_i, t\right) \right] \Delta z \quad (3)$$

where $G_{ITHP,0}$ is the ground heat flux (W/m^2), $\rho_s c_s$ is the soil heat capacity (J/(m^3·K)), and $T(z,t)$ is the measured soil temperature (°C). This method of estimating ground heat flux is a combination of HFP01SC measurements and the integral method, and is called ITHP for the convenience of description in this study.

2.3. Harmonic analysis

Molecular conduction dominates the heat transfer process in the soil (Stull, 1988). The heat flux by conduction vertically through the soil (G) is proportional to the vertical gradient of soil temperature and is given as:

$$G = -\lambda_s \frac{\partial T}{\partial z} \quad (4)$$

where T is the soil temperature (°C), λ_s (W/(m·K)) is the soil thermal conductivity, and z (m) is the soil depth (positive downward). Neglecting any horizontal heat conduction in the soil, *i.e.*, assuming no other heat source/sink in the soil, the one-dimensional soil thermal diffusion equation can be given as:

$$\frac{\partial T}{\partial t} = -\frac{1}{\rho_s c_s} \frac{\partial G}{\partial z} \quad (5)$$

If the soil moisture does not change with depth or the change is so small that its impact on the thermal parameters, $\rho_s c_s$ and λ_s, can be neglected, these two parameters can be considered as constant for a homogeneous soil. Assuming that there is only vertical heat transfer, equation *(5)* can be simplified as:

$$\frac{\partial T}{\partial t} = \kappa \frac{\partial^2 T}{\partial z^2} \quad (6)$$

where $\kappa=\lambda_s/\rho_s c_s$ (m^2/s) is the soil thermal diffusivity. The initial and boundary conditions are given as:

$$t=0,\ \ T(z)=T_0-\gamma z,\ \ z\geq 0 \tag{7a}$$

$$z=0,\ \ T(t,0)=T_0+\sum_{n=1}^{M}A_{0n}\sin(n\omega t+\theta_{0n}),\ \ t>0 \tag{7b}$$

where n is the harmonic wave number, ω ($=2\pi/N$) is the radial frequency, N is the total number of samples, M is the highest harmonic wave number, A_0 and θ_0 are the amplitude and the phase, and γ (K/m) is the soil temperature lapse rate with depth. Then the analytical solution of equation *(6)* can be obtained by using the variable separation method as follows:

$$T(z,t)=T_0-\gamma z+\sum_{n=1}^{M}A_{0n}\exp(-Bz)\sin(n\omega t+\theta_{0n}-Bz) \tag{8}$$

where $B=\sqrt{n\omega/2\kappa}$. If z is so small that the effect of γz on the soil temperature can be neglected, it is acceptable to assume that the mean soil temperatures at all levels are uniform, *i.e.*, $\gamma z\approx 0$. Then the analytical solution becomes:

$$T(z,t)=T_0+\sum_{n=1}^{M}A_{0n}\exp(-Bz)\sin(n\omega t+\theta_{0n}-Bz) \tag{9}$$

By taking the derivative $\partial T/\partial z$ of equation *(9)* and multiplying this by λ_s (or $\rho_s c_s/\kappa$), the soil heat flux G(z,t) can be given as:

$$G(z,t)=\frac{\rho_s C_s}{\kappa}\sum_{n=1}^{M}\left[A_{0n}\sqrt{\frac{n\omega}{\kappa}}\exp(-Bz)\cdot \sin\left(n\omega t+\theta_{0n}+\frac{\pi}{4}-Bz\right)\right] \tag{10}$$

The soil heat capacity can be calculated with the following formula:

$$\rho_s c_s=\rho_d c_d(1-Q_{sat})+\rho_w c_w Q \tag{11}$$

where Q (m^3/m^3) is the soil water content, Q_{sat} is the soil porosity and has an observed value of 0.53 at the SACOL site, $\rho_w c_w=4.19\times10^6$ J/($m^3\cdot$K) is the heat capacity of liquid water, and $\rho_d c_d$ is the heat capacity of the dry soil (J/($m^3\cdot$K)), which can be determined from the observations. Therefore, the soil heat flux at a certain depth can be calculated from the observed soil temperature according to equation *(10)*. The soil thermal diffusivity κ can be estimated from a fit of equation *(9)* into the measured soil temperature. This method of estimating soil heat flux is called HA (harmonic analysis technique) in this study.

2.4. TDEC method

By integrating equation *(5)*, the soil heat flux G(z) can be expressed as:

$$G(z)=G(z_{ref})+\int_{z_{ref}}^{z}\frac{\partial\rho_s c_s T(z)}{\partial t}dz \tag{12}$$

where $G(z_{ref})$ is the soil heat flux at a reference depth (z_{ref}). Given temperature profile $T(z_i)$, the discretized form of equation *(12)* is:

$$G(z,t)=G(z_{ref},t)+\frac{1}{\Delta t}\sum_{z_{ref}}^{z}\left[\rho_s c_s\cdot(z_i,t+\Delta t)\cdot T(z_i,t+\Delta t)-\rho_s c_s(z_i,t)T(z_i,t)\right]\Delta z \tag{13}$$

If the reference level z_{ref} is so deep that $G(z_{ref})$ is much less than the ground heat flux, it is acceptable to assume $G(z_{ref})\approx 0$. According to equation *(11)*, the heat capacity can be calculated from soil water content and soil porosity, which can be easily determined. Therefore, the key issue in calculating the ground heat flux with equation *(13)* is how to make a reliable soil temperature profile from limited observations. Recently, Yang and Wang (2008) developed a new interpolation method of making the soil temperature profile. By assuming a constant soil thermal conductivity (*e.g.*, 1.0 W/(m·K)), they calculated the basic profile of soil temperature (T_{TDEC}) with the soil thermal diffusion equation. Then the temperature errors due to inaccurate soil thermal conductivity were corrected by the observations. Finally, soil heat flux at all layers can be obtained by integrating equation *(13)* from the bottom to the surface. This new method, called TDEC, is simple and can be easily realized (Yang and Wang, 2008).

3. Results

In order to eliminate the influence of rainfall/snow on the result, a dataset of only 11 days (from July 17 to 27, 2008) was selected for a detailed analysis in this study. During this 11-day period, the soil temperature in the middle and upper layers was characterized by significant diurnal variation and decreased amplitude with depth. The range of soil temperature at the ground surface was 11.3 ºC to 54.0 ºC, which was significantly larger than that from 15.8 ºC to 39.6 ºC at a depth of 2 cm, indicating a more dramatic change of soil temperature in the upper layer. The soil temperature at the deeper layer varied little with time, especially at a depth of 80 cm which was nearly constant (data not shown). The mean soil temperature at depths of 2 cm, 5 cm, and 10 cm were 26.3 ºC, 25.9 ºC, and 25.5 ºC, respectively, indicating nearly uniform mean temperature in vertical in the upper soil layer. Moreover, the soil water content in all layers varied little with time and was constant (6.7 percent) at a depth of 80 cm. The ranges of soil water content at depths of 5 cm and 10 cm were 9.5 to 11.5 percent and 11.0 to 12.5 percent, respectively.

Moreover, some of the definitions used in this study are given as follows: $T_{i,L}$ and $G_{i,L}$ indicate the soil temperature and soil heat flux, respectively, at a depth of L cm, where i

indicates the approach to estimate the soil heat flux, *i.e.*, TDEC, HA, or ITHP; Obs represented observation. We also defined the root mean square (rms) and bias, respectively, between two time series x and y as follows:

$$\text{rms} = \sqrt{\frac{1}{N}\sum_{j=1}^{N}\left(x_j - y_j\right)^2} \tag{14a}$$

$$\text{bias} = \left|\frac{1}{N}\sum_{j=1}^{N}\left(x_j - y_j\right)\right| \tag{14b}$$

3.1. Determination of soil thermal parameters

The HA technique and the integral method both require the soil heat capacity $\rho_s c_s$ (or the heat capacity of dry soil $\rho_d c_d$) in the calculation of soil heat flux. The former also requires the soil thermal diffusivity κ, which can be estimated by fitting equation *(9)* into the measured soil temperature. A detailed description of the calculation of κ can be found in the report by Heusinkveld *et al*. (2004).

Figures 1(a) and 1(b) compare the fitting of soil temperature with HA and the observed soil temperatures at depths of 5 cm and 10 cm, respectively. It is shown that the fitting and the observed soil temperatures had almost a 1:1 linear relationship with each other (R^2 = 1.00). Their rms and bias were about 0.20 °C and 0.08 °C, respectively, at 5 cm depth, and 0.33 °C and 0.18 °C, respectively, at 10 cm depth. This indicates that the soil temperature in the upper layer can be accurately fitted with HA at the SACOL site. With a mean soil water content of about 11 percent, the soil thermal diffusivity estimated with HA is about 7.2×10^{-7} m^2/s at this site.

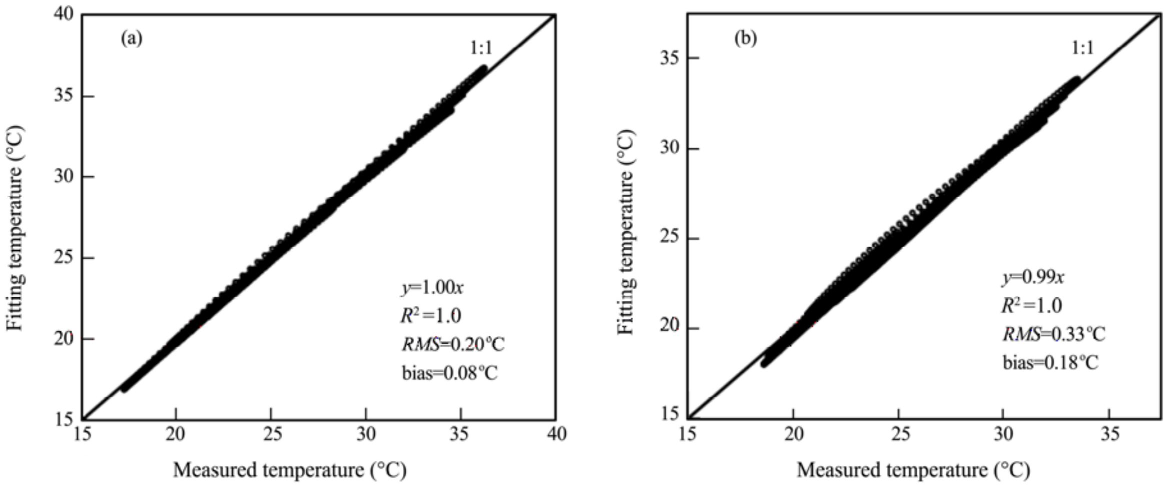

Figure 1 Comparisons of fitting soil temperatures with the HA technique and the observed soil temperatures (Obs) at depths of (a) 5 cm and (b) 10 cm, respectively

The soil thermal conductivity λ_s can be obtained by fitting equation *(4)* to the observed soil heat flux and the vertical gradient of the soil temperature. Figure 2 shows the distributions of the observed soil heat flux at a depth of 5 cm ($G_{Obs,5}$) and the observed vertical gradient of soil temperatures between depths of 2 cm and 10 cm (dT/dz). It is shown that the soil heat flux was highly correlated with the vertical gradient of soil temperature (R^2 = 0.99). According to equation *(4)*, the slope of the regression line in figure 2 can represent the soil thermal conductivity λ_s. This indicates that a λ_s of about 1.0 W/(m·K) was obtained at the SACOL site, which was greater than that of the heat flux plate (λ_m = 0.8 W/(m·K)). Then the soil heat capacity can be estimated from the well known λ_s and κ according to their relationship, *i.e.*, $\kappa = \lambda_s/\rho_s c_s$. With a mean soil water content of 11 percent, the soil heat capacity is about 1.4×10^6 J/(m^3·K) at the SACOL site, which indicates that the heat capacity of dry soil ($C_d = \rho_d c_d(1 - Q_{sat})$) at this site is about 0.9×10^6 J/(m^3·K).

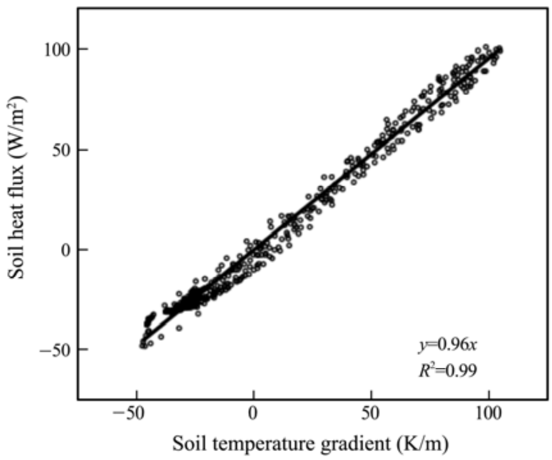

Figure 2 Scattergram of the observed soil heat flux at a depth of 5 cm versus the observed vertical gradient of soil temperatures between depths of 2 cm and 10 cm. The line is the linear fit for all the data.

Harmonic analysis requires a vertical homogenous soil for performing soil thermal analysis. Therefore, we examined whether the soil at the SACOL site met this condition. As shown in Table 1, the soil bulk density (ρ_d), with a range of 1.20×10^3 to 1.22×10^3 kg/m^3 between surface and 100 cm depth, varies little with depth at the SACOL site. The soil porosity (Q_{sat}) depends on the soil bulk density and the soil weight (D), *i.e.*, $Q_{sat} = 1 - \rho_d/D$. With a measurement value of $D = 2.6$, the soil porosities calculated from the above soil bulk densities had a range of about 0.52 to 0.54, indicating little variation of soil porosity with depth at this site. This indicates that the soil is nearly homogenous in vertical at the SACOL site, which can meet the requirement of HA in performing soil thermal analysis.

Table 1 Soil bulk density (ρ_d) of different soil layers at the SACOL site*

Layer (cm)	0–10	10–20	20–30	30–40	40–60	60–80	80–100
ρ_d (g/cm^3)	1.22	1.21	1.20	1.22	1.24	1.24	1.24

*From Li *et al.*, 2008.

3.2. Comparisons of soil heat fluxes calculated with different approaches

According to equation *(10)* or equation *(13)*, soil heat flux at a certain depth can be calculated from observations by using the HA technique or the TDEC method. In addition, soil heat flux at a depth of 5 cm could be measured with an HFP01SC self-calibrating heat flux plate at the SACOL site. Ground heat flux can also be estimated by summing the HFP01SC measurements and the soil heat storage between the plate and the ground surface. The following section presents a comparison analysis of the soil heat flux determined with these different approaches.

Figures 3(a) and 3(b) show the comparisons of soil heat flux measured with an HFP01SC heat flux plate and those calculated with the HA technique and the TDEC method, respectively, at a depth of 5 cm. It is shown that the heat fluxes calculated with the HA technique ($G_{HA,5}$) and with the TDEC method ($G_{TDEC,5}$) were both highly correlated with the measured heat flux ($G_{Obs,5}$) (R^2 of about 0.98 and 0.99, respectively). However, $G_{HA,5}$ and $G_{TDEC,5}$ were both slightly larger than $G_{Obs,5}$, by about 2 percent and 6 percent, respectively. $G_{HA,5}$ and $G_{TDEC,5}$ were closer to each other, with a slope of linear regression as high as 1.0 and $R^2 = 0.98$ (data not shown).

The sign and phase of soil heat fluxes measured with a heat flux plate are usually considered to be accurate (*e.g.*, Yang and Wang, 2008), so they can be used as a reference for the validation of the soil heat fluxes estimated with other methods. Figure 4 shows the measured and calculated soil heat fluxes at a depth of 5 cm at the SACOL site. For a better visualization, only 6 days (DOYs from 204 to 210, 2008) are shown. These data demonstrate that the soil heat fluxes calculated with the HA technique and the TDEC method both follow the sign and phase of the HFP01SC measurements very well, indicating that both HA and TDEC likely have only small errors in the phase of the estimated soil heat fluxes. In particular, the time curves of the soil heat fluxes calculated with the HA technique and the TDEC method almost overlap. However, the absolute HFP01SC measurements were significantly smaller than those calculated with the HA technique and the TDEC method during the nighttime, resulting in a relatively large difference between the calculated and the measured soil heat fluxes.

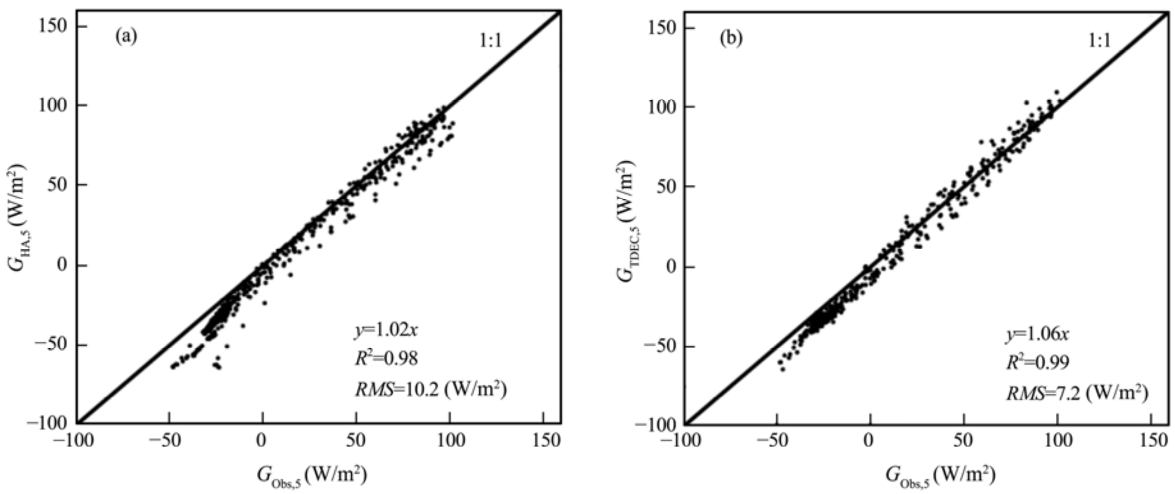

Figure 3 Comparisons of the soil heat fluxes measured with an HFP01SC heat plate ($G_{Obs,5}$) and calculated with (a) the HA technique ($G_{HA,5}$) and (b) the TDEC method ($G_{TDEC,5}$) at a depth of 5 cm at the SACOL site

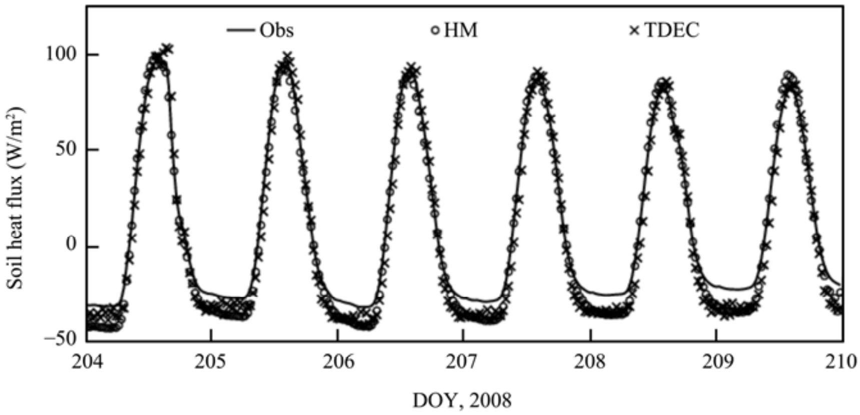

Figure 4 Soil heat fluxes measured with an HFP01SC heat plate (Obs) and calculated with the HA technique and the TDEC method, respectively, at a depth of 5 cm for DOYs from 204 to 210, 2008

The accurate estimation of ground heat flux is important, especially for surface energy budget studies. Figure 5 compares ground heat fluxes calculated with different approaches. There is a nearly 1:1 linear relationship between the ground heat fluxes calculated with the TDEC method ($G_{TDEC,0}$) and the HA technique ($G_{HA,0}$) ($R^2 = 0.97$ and a bias of about 1.9 W/m^2) (Figure 5(a)). The former also has good agreement with the ground heat flux calculated with the ITHP approach ($G_{ITHP,0}$) ($R^2 = 0.99$ and a bias of about 4.6 W/m^2), but $G_{TDEC,0}$ is larger than $G_{ITHP,0}$ by about 9 percent (Figure 5(b)). The sign and phase of the ground heat fluxes calculated with these three approaches agree well with each other and their time curves almost overlap (data not shown). However, the absolute $G_{ITHP,0}$ is slightly smaller than the absolute $G_{TDEC,0}$ and the absolute $G_{HA,0}$ during the nighttime, which mainly resulted from the smaller absolute measurements with the HFP01SC at the depth of 5 cm.

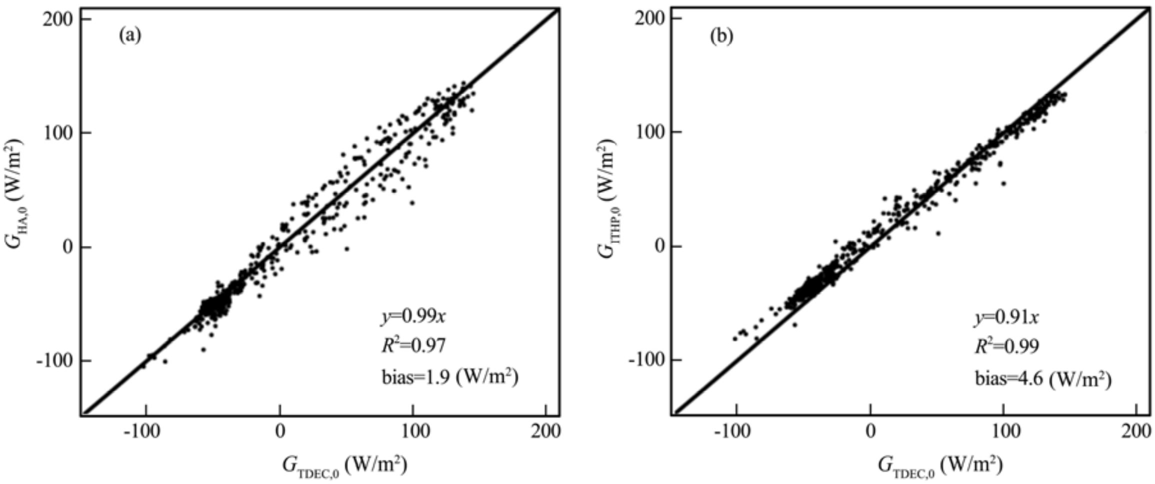

Figure 5 Comparisons of ground heat fluxes calculated with the TDEC method ($G_{TDEC,0}$) and (a) the HA technique ($G_{HA,0}$) and (b) the ITHP approach involving HFP01SC measurement

3.3. Impact of the ground heat flux on the surface energy budget

Due to the important role of ground heat flux (G_0) in the surface energy balance, many studies have focused on the characteristics of the G_0 component and its contribution to the surface energy budget over the Loess Plateau of northwest China in recent years (Yang *et al*., 2004b; Wei *et al*., 2005; Liu *et al*., 2007; Wang *et al*., 2007; Wen *et al*., 2007). Among these studies, measurements with a heat flux plate buried at a certain depth below the ground surface were usually used as the G_0 component of the surface energy balance without extrapolating to the ground surface (*e.g*., Yang *et al*., 2004b; Wei *et al*., 2005; Wang *et al*., 2007). For the surface energy budget, however, the soil heat storage (S) in the layer between the heat flux plate and the ground surface could not be neglected and a higher energy budget closure could be obtained if the S term is taken into account (*e.g*., Jacobs *et al*., 2007; Liu *et al*., 2007).

The previous results have shown that the soil heat fluxes calculated with the HA technique and the TDEC method both agree well with the HFP01SC measurements at the SACOL site. Ground heat fluxes can be calculated with any of these approaches, *i.e.*, HA, TDEC, and ITHP involving HFP01SC measurements, and then used to evaluate the closure of the surface energy budget.

The simplified surface energy balance equation can be expressed as:

$$R_n - G_0 = \lambda E + H \quad (15)$$

where R_n is the net radiation (W/m^2), calculated from the upward and downward longwave and shortwave radiation components, and λE and H are the latent and sensible heat fluxes (W/m^2), respectively. In addition, the closure of the surface energy budget is defined as:

$$\alpha = \frac{\lambda E + H}{R_n - G_0} \quad (16)$$

In this study, α was determined with the least squares method.

Figure 6 shows the variations of the surface energy balance components during an almost clear day at the SACOL site. The turbulent fluxes, including λE and H, and the ground heat flux were all positive during the daytime, indicating that the former were transported upward into the atmosphere and the latter downward into the soil. In contrast, during the nighttime the sensible heat flux was transported downward and the ground heat flux upward to the surface, while the latent heat transfer was very weak. Furthermore, it is also shown that the sensible heat transfer played a major role and the soil heat flow and latent heat transfer were secondary in the consumption of the net radiation during the daytime.

Table 2 shows that the characteristics of surface energy balance depended on different methods of estimating ground heat flux at the SACOL site. To eliminate the influence of eddy covariance flux uncertainty during the nighttime (Massman and Lee, 2002), only data collected during the daytime were used in this analysis. It is shown that a closure of only about 76 percent was obtained by using the direct measurements with an HFP01SC heat flux plate buried at a depth of 5 cm ($G_{Obs,5}$) in the estimation of surface energy budget closure. By using the TDEC-calculated ground heat flux $G_{TDEC,0}$ instead of $G_{Obs,5}$, the closure was about 83 percent, an improvement of 7 percent. Moreover, the contributions of H, λE, and $G_{TDEC,0}$ to the surface energy budget were about 47 percent, 20 percent, and 21 percent of R_n, respectively, while $G_{Obs,5}$ was only about 13 percent of R_n. If the HFP01SC measurements were extrapolated to the ground surface, the proportion of soil heat flux to the net radiation was improved by about 7 percent and the associated surface energy budget closure improved by about 6 percent. The ground heat flux calculated with the HA technique was about 20 percent of R_n and could result in a surface energy budget closure of about 82 percent, which was also higher than the closure (76 percent) estimated from the HFP01SC measurements without fully taking the soil heat storage into account. These results indicate that the soil heat storage in the layer between the flux heat plate and the ground surface was about 7 to 8 percent of R_n at the SACOL site. If this part of the heat storage was taken into account, the surface energy budget closure would be improved by 6 to 7 percent.

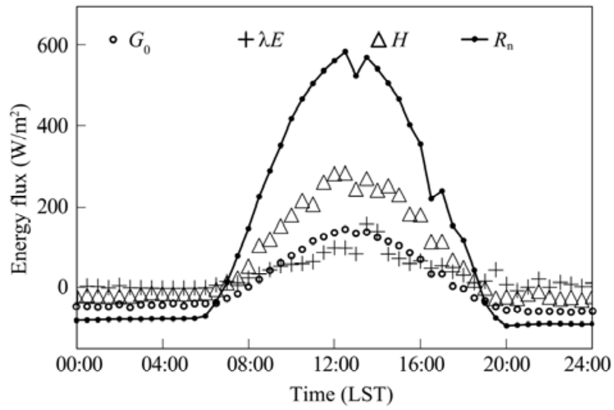

Figure 6 Measurements of the surface energy balance components during an almost clear day. R_n indicates the net radiation flux, H and λE the sensible and latent heat fluxes, respectively, measured with the eddy covariance technique, and G_0 is the TDEC-calculated ground heat flux.

Therefore, the ground heat flux has a very important contribution to the surface energy budget for the semi-arid grassland over the Loess Plateau mesa region. The surface energy budget closure was improved significantly when the soil heat storage was fully taken into account at the SACOL site. Even by doing so, the resultant imbalance was still about 49.7 to 52.9 W/m^2. The reasons for this imbalance will be further discussed in another study.

Table 2 Dependence of characteristics of surface energy balance on different methods of estimating ground heat flux (G_0) at the SACOL site

Method	G_0/R_n	α	R^2	ΔE
TDEC	0.21	0.83	0.88	49.7
HA	0.20	0.82	0.88	52.9
ITHP	0.20	0.82	0.88	52.0
HFP01SC[a]	0.13	0.76	0.89	74.8

[a]The HFP01SC heat flux plate was buried at a depth of 5 cm. R_n indicates the net radiation, α the closure rate of the surface energy budget, R the linear correlation coefficient between the sum of sensible and latent heat fluxes ($H + \lambda E$) and the surface available energy ($R_n - G_0$), and $\Delta E = R_n - (\lambda E + H + G_0)$, the residual energy flux (W/m^2).

4. Conclusions and discussion

Three methods of estimating ground heat flux were evaluated and the impact of their calculated results on the surface energy budget was analyzed by using observations from the Semi-Arid Climate and Environment Observatory of Lanzhou University (SACOL) in July, 2008. These approaches included the HA technique, the TDEC method, and the calorimetric method involving soil heat flux measurement with a self-calibrating heat flux plate (Model HFP01SC). It was shown that the soil heat fluxes calculated with the HA technique and the TDEC method were both highly correlated with the soil heat flux measured with the HFP01SC heat flux plate. In addition, these calculated soil heat fluxes well followed the sign and phase of the HFP01SC measurements, and the magnitude of the former was close to that of the latter. Furthermore, ground heat flux calculated with any of these approaches (HA, TDEC, and the calorimetric method) can be used to assess the closure of surface energy budget at the SACOL site. By fully taking the soil heat storage into account, a closure of about 82 to 83 percent was obtained, an improvement of about 6 to 7 percent compared to the HFP01SC direct measurements at a depth of 5 cm.

In the estimation of ground heat flux, the HA technique only requires soil temperature at the surface or in a layer near the surface, and the relevant soil thermal parameters. However, HA assumes that the soil temperature could be described with a sine function or a Fourier series, which may be far from the reality. This method also assumes a vertical homogenous soil, implying that a homogenous or nearly homogenous soil is required in soil thermal analysis (Heusinkveld *et al*., 2004).

TDEC is a type of integral method of estimating soil heat flux from observations of multi-level soil temperature and soil moisture. An obvious advantage of TDEC is its insensitivity to the soil thermal conductivity, which is difficult to determine accurately (Yang and Wang, 2008). Because the soil temperatures in the upper soil layer always have dramatic variations, large vertical gradients, and significant differences in phase between different levels, a reliable temperature profile calculated from limited observations is crucial for estimating soil heat flux with the integral method. Unlike the general integral method, TDEC uses the soil thermal diffusion equation to construct the major part of the temperature profile, and then a linear interpolation to correct minor errors of this profile, resulting in a more reliable temperature profile for estimating soil heat flux. Our results showed that soil heat flux calculated with the TDEC method agreed well with that calculated with the HA technique. These calculated results were both close to the HFP01SC measurements, indicating that the TDEC method may be a reliable and effective method of estimating ground heat flux.

Direct measurement with a heat flux plate is a relatively simple method of determining soil heat flux. However, measurements taken with a common heat flux plate usually have large errors in their magnitude that are difficult to calibrate accurately by post-processing (van Loon *et al*., 1998). The HFP01SC self-calibrating heat flux plate is different from other types of heat flux plates in that it can provide a more accurate estimation of soil heat flux in laboratory studies as well as in field experiments (van Loon *et al*., 1998; Ochsner *et al*., 2006). Although Cobos and Baker (2003) found that the soil heat flux measured with an HFP01SC heat flux plate was overestimated by about 22 percent in the laboratory, the HFP01SC measurements were shown to be reliable in their field study. Our field study also showed that the HFP01SC measurements were likely accurate at the SACOL site. Therefore, the calorimetric method involving HPF01SC measurements may also be a reliable and effective method of estimating ground heat flux.

Acknowledgments:
We would like to thank the two anonymous reviewers for their insightful comments and suggestions which further improved the quality of the manuscript. We are grateful for the script provided by Prof. Yang Kun to calculate soil heat flux with the TDEC method. This project was supported by the National Natural Science Foundation of China (Grant No. 40725015).

REFERENCES

Cobos DR, Baker JM, 2003. In situ measurement of soil heat flux with the gradient method. Vadose Zone Journal, 2: 589–594.

Culf AD, Foken T, Gash JHC, 2004. The energy balance closure problem. In: Kabat P, Claussen M (eds.), Vegetation, Water, Humans and the Climate: A New Perspective on an Interactive System. Springer, Berlin. 159–166.

Fan X, Tang M, 1994. A preliminary study on conductive and convective soil heat flux. Plateau Meteorology, 13(1): 14–19.

Foken T, 2008. The energy balance closure problem: an overview. Ecological Applications, 18: 1351–1367.

Gao Z, Fan X, Bian L, 2003. An analytical solution to one-dimensional thermal conduction-convection in soil. Soil Science, 168: 99–107.

Heusinkveld BG, Jacobs AFG, Holtslag AAM, Berkowicz SM, 2004. Surface energy balance closure in an arid region: role of soil heat flux. Agricultural and Forest Meteorology, 122: 21–37.

Horton R, Wierenga PJ, Nielsen DR, 1983. Evaluation of methods for determining the apparent thermal diffusivity of soil near the surface. Soil Science Society of America Journal, 47: 25–32.

Huang J, Zhang W, Zuo J, Bi J, Shi J, Wang X, Chang Z, Huang Z, Yang S, Zhang B, Wang G, Feng G, Yuan J, Zhang L, Zuo H, Wang S, Fu C, Chou J, 2008. An overview of the semi-arid climate and environment research observatory over the Loess Plateau. Advances in Atmospheric Sciences, 25(6): 906–921.

Hukseflux Thermal Sensors, 1999. Application and specification of heat flux sensors, v. 9904. Hukseflux Thermal Sensors, Delft, The Netherlands, 16, www.hukseflux.com/downloads/thermalScience/applicAndSpec.pdf.

Jacobs AFG, Heusinkveld BG, Holtslag AAM, 2007. Towards closing the surface energy budget of a mid-latitude grassland. Boundary-Layer Meteorology, 126: 125–136.

Li X, Fu H, Li X, Guo D, Dong X, Wan C, 2008. Effects of land-use regimes on carbon sequestration in the Loess Plateau, Northern China. New Zealand Journal of Agricultural Research, 51: 45–52.

Li Z, Yu G, Wen X, Zhang L, Ren C, Fu Y, 2005. Energy balance closure at China FLUX sites. Science in China Series D: Earth Sciences, 48: 51–62.

Liebethal C, Huwe B, Foken T, 2005. Sensitivity analysis for two ground heat flux calculation approaches. Agricultural and Forest Meteorology, 132: 253–262.

Liu Y, Wen J, Wei Z, Li Z, Zhang T, Liu R, 2007. Observation and analysis of the land surface radiation and energy balance over the Loess Plateau Mesa region. Plateau Meteorology, 26(5): 928–937.

Massman WJ, Lee X, 2002. Eddy covariance flux corrections and uncertainties in long term studies of carbon and energy exchanges. Agricultural and Forest Meteorology, 113: 121–144.

Ochsner TE, Sauer TJ, Horton R, 2007. Soil heat storage measurements in energy balance studies. Agronomy Journal, 99: 311–319.

Ochsner TE, Sauer TJ, Horton R, 2006. Field tests of the soil heat flux plate method and some alternatives. Agronomy Journal, 98: 1005–1014.

Oncley SP, Foken T, Vogt R, Kohsiek W, DeBruin HAR, Bernhofer C, Christen A, van Gorsel E, Grantz D, Feigenwinter C, Lehner I, Liebethal C, Liu H, Mauder M, Pitacco A, Ribeiro L, Weidinger T, 2007. The energy balance experiment EBEX-2000. Part I: overview and energy balance. Boundary-Layer Meteorology, 123: 1–28.

Stull RB, 1988. An Introduction to Boundary Layer Meteorology. Kluwer Academic, Norwell, MA. 274–287.

Tanaka K, Tamagawa I, Ishikawa H, Ma Y, Hu Z, 2003. Surface energy budget and closure of the eastern Tibetan Plateau during the GAME-Tibet IOP 1998. Journal of Hydrology, 283: 169–183.

van Loon WKP, Bastings HMH, Moors EJ, 1998. Calibration of soil heat flux sensors. Agricultural and Forest Meteorology, 92: 1–8.

Wang C, Huang B, Yang X, 2007. A study on surface flux and the bulk transfer coefficients over middle Gansu region of Loess Plateau under the wheat and bare fields. Plateau Meteorology, 26(1): 30–38.

Wei Z, Wen J, Lü S, Chen S, Ao Y, Liang L, 2005. A primary field experiment of land-atmosphere interaction over the Loess Plateau and its ground surface energy in clear day. Plateau Meteorology, 24(4): 545–555.

Wen J, Wei Z, Lü S, Chen S, Ao Y, Liang L, 2007. The characteristics of land surface energy and water exchange over the Loess Plateau Mesa in China. Advances in Atmospheric Sciences, 24(2): 301–310.

Wilson KB, Goldstein A, Falge E, Aubinet M, Baldocchi D, Berbigier P, Bernhofer C, Ceulemans R, Dolman H, Field C, Grelle A, Ibrom A, Law BE, Kowalski A, Meyers T, Moncrieff J, Monson R, Oechel W, Tenhunen J, Valentini R, Verma S, 2002. Energy balance closure at FLUXNET sites. Agricultural and Forest Meteorology, 113: 223–243.

Yang K, Koike T, Ishikawa H, Ma Y, 2004a. Analysis of the surface energy budget at a site of GAME/Tibet using a single-source model. Journal of the Meteorological Society of Japan, 82: 131–153.

Yang K, Wang J, 2008. A temperature prediction-correction method for estimating surface soil heat flux from soil temperature and moisture data. Science in China Series D: Earth Sciences, 51(5): 721–729.

Yang X, Zhang Q, Wang R, Ma P, Yang Q, Liu H, 2004b. Experimental study on surface energy balance over Loess Plateau of middle part Gansu in summer. Plateau Meteorology, 23(6): 828–834.

Zhang L, Jiang H, Li L, 2006. A test of the soil heat flux calculation in Wudaoliang area using meteorological elements. Plateau Meteorology, 25(3): 418–422.

Zhang L, Jiang H, Li L, 2004. Study of calculation of soil heat conduction: progress and prospect. Journal of Glaciology and Geocryology, 26(5): 569–575.

Zuo J, Huang J, Wang J, Zhang W, Bi J, Wang G, W Li, Fu P, 2009. Surface turbulent flux measurements over the Loess Plateau for a semi-arid climate change study. Advances in Atmospheric Sciences, 26(4): 1–13.